Electronic Supplementary Material (ESI) for Biomaterials Science.
This journal is © The Royal Society of Chemistry 2022

Title page:

Engineering goat milk-derived extracellular vesicles for multiple bioimaging-guided and photothermal-enhanced therapy of colon cancer

Boping Jing[1,2,3†], Yu Gao[1,3†], Feng Guo[4], Dawei Jiang[1,3], Rong Guo[1,3], Jing Wang[2,3], Yuman Li[2,3], Yuji Xie[2,3] , Yihan Chen[2,3], He Li[2,3], Li Zhang[2,3*], Mingxing Xie[2,3*], Rui An[1,3*]

Affiliations

[1]Department of Nuclear Medicine, Union Hospital, Tongji Medical College, Huazhong University of Science and Technology, Wuhan 430022, China

[2]Department of Ultrasound Medicine, Union Hospital, Tongji Medical College, Huazhong University of Science and Technology, Wuhan 430022, China

[3]Hubei Key Laboratory of Molecular Imaging, Wuhan 430022, China

[4]Department of Pancreatic Surgery, Union Hospital, Tongji Medical College, Huazhong University of Science and Technology, Wuhan 430022, China

† **Boping Jing and Yu Gao contributed equally to this work**

***Corresponding Authors:**

Rui An, No. 1277 Jiefang Ave, Wuhan, Hubei Province 430022, China. Phone: +86-13986113240; Fax: +86-27-87543437. E-mail: 1975xh0577@hust.edu.cn

Mingxing Xie, No. 1277 Jiefang Ave, Wuhan, Hubei Province 430022, China. Phone: +86-13607108938; Fax: +86-27-85726172. E-mail: xiemx@hust.edu.cn

Li Zhang No. 1277 Jiefang Ave, Wuhan, Hubei Province 430022, China. Phone: +86-18907131488; Fax: +86-27-85726172. E-mail: zli429@hust.edu.cn

Figure S1

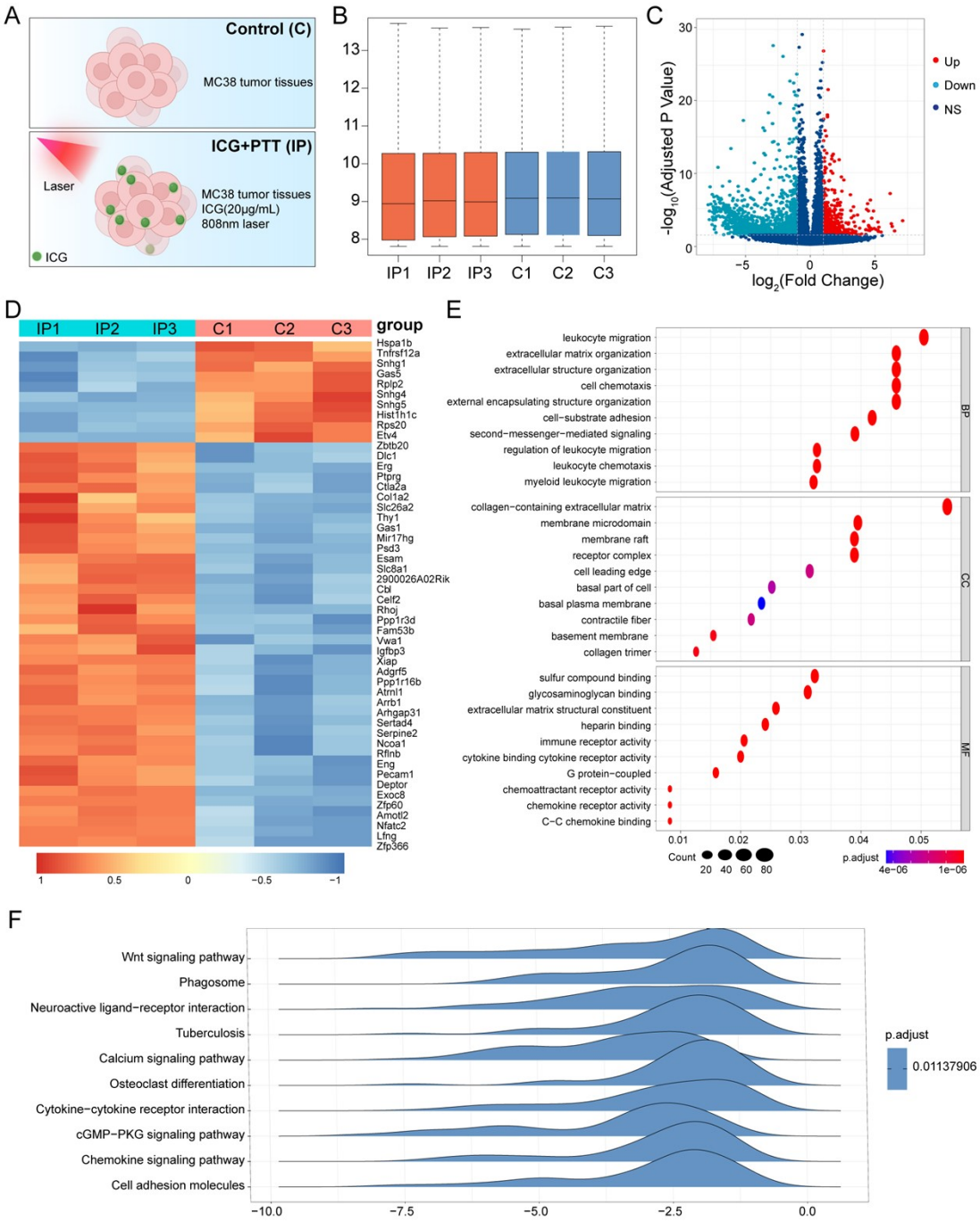

Figure S1. Bioinformatics analysis of the antitumor effect of PTT. (A) MC38 tumor tissues with or without PTT were used for RNA-seq analysis. (B) The analysis of the quality control of RNA sequencing. (C) The change in the number of genes after PTT. (D) Significant changes in the expression levels of genes. (E) Changes of many biological processes after PTT. (F) Changes of significant signaling pathways after PTT.

Figure S2

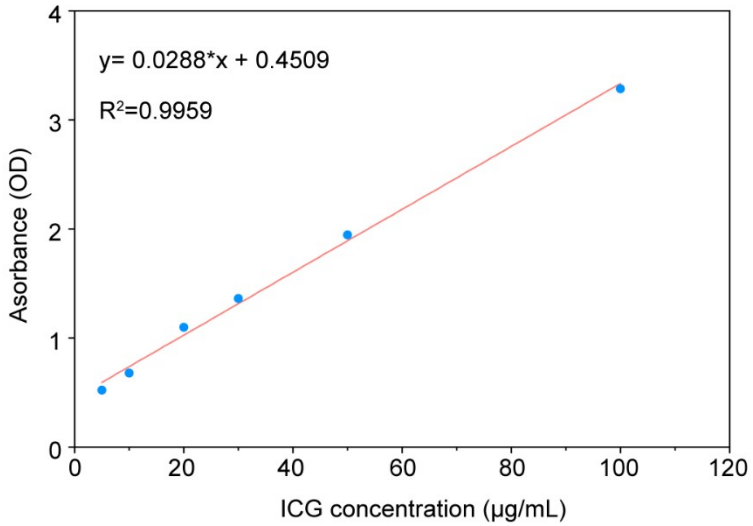

Figure S2. ICG standard concentration-absorbance curve at 790 nm.

Figure S3

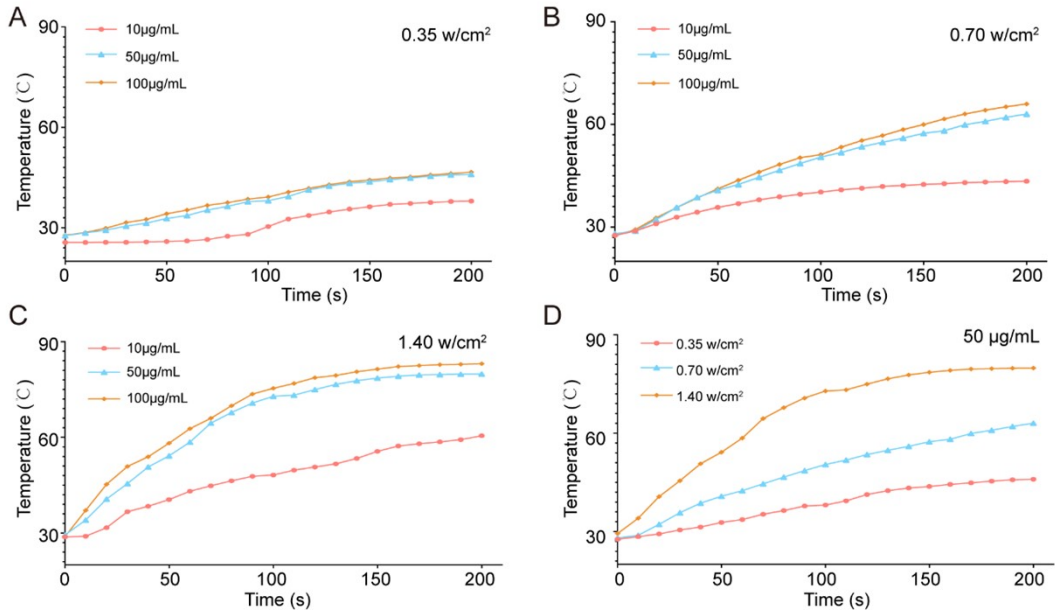

Figure S3. *In vitro* temperature curves of different concentrations of ICG or laser power densities. (A) *In vitro* temperature curves of different concentrations of ICG at the laser power density of 0.35 w/cm^2. (B) *In vitro* temperature curves of different concentrations of ICG at the laser power density of 0.70 w/cm^2. (C) *In vitro* temperature curves of different concentrations of ICG at the laser power density of 1.40 w/cm^2. (D) *In vitro* temperature curves of different laser power densities.

Figure S4

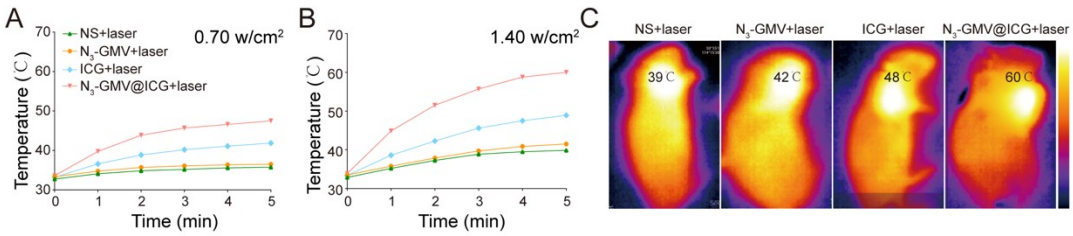

Figure S4. *In vivo* photothermal performance. (A) *In vivo* temperature curves of tumors treated with normal saline (NS), ICG solution, GMV solution and N_3-GMV@ICG solution at the laser power density of 0.70 w/cm^2 for 5 min. (B) *In vivo* temperature curves of tumors at the laser power density of 1.40 w/cm^2 for 5 min. (C) Infrared thermal imaging of tumors at the laser power density of 1.40 w/cm^2 for 5 min.

Figure S5

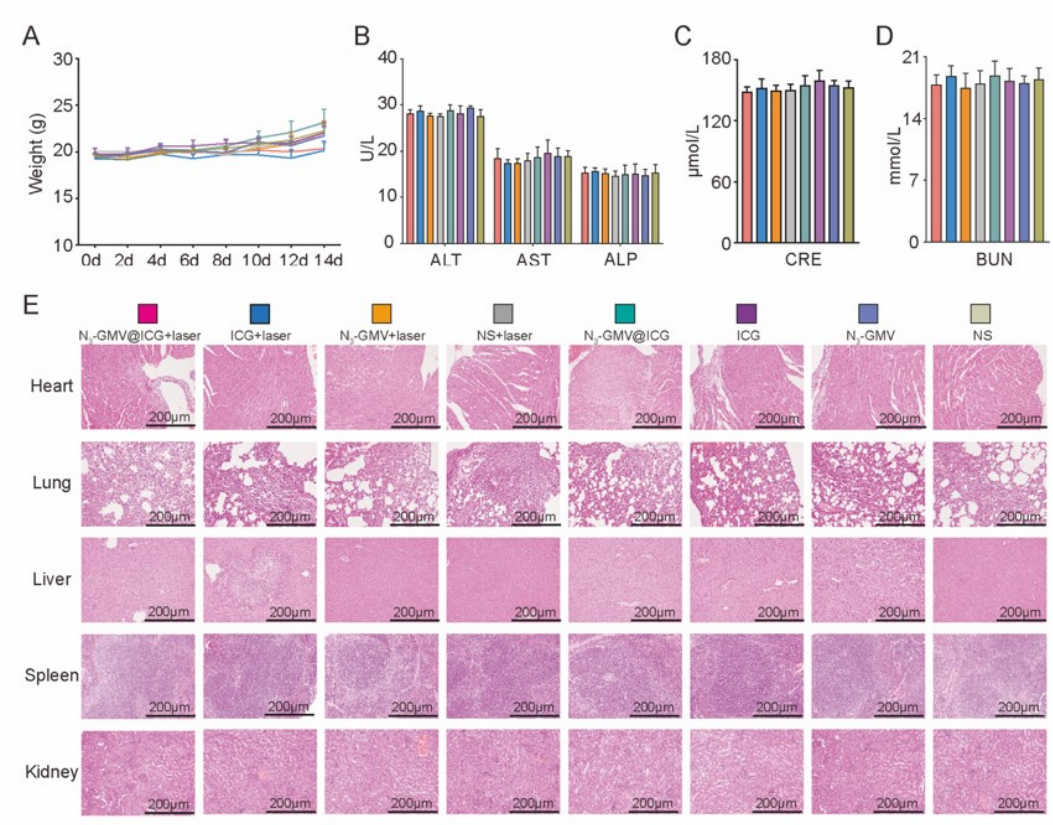

Figure S5. *In vivo* toxicity evaluation by blood test and histology analysis. (A) Body weight change curves, n=5. (B-D) Liver function makers (ALT, AST and ALP) and kidney function markers (BUN and CRE) after different treatment over 14 d. (E) Representative H&E staining images of major organs from the euthanized mice. Bar = 200 μm. Data are represented as mean ± standard deviation (n = 6).

Figure S6

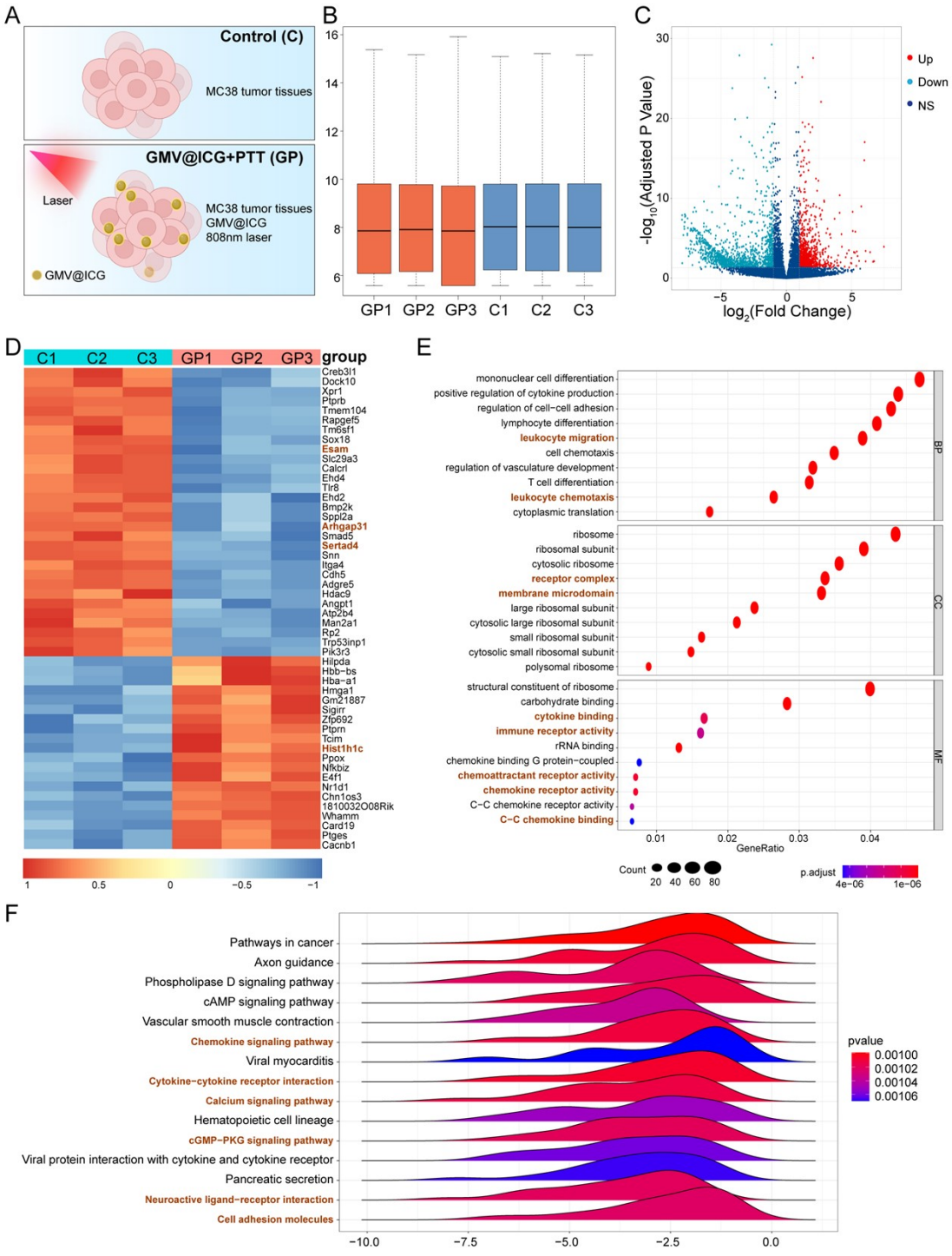

Figure S6. Bioinformatics analysis of the antitumor effect of PTT based on N_3-GMV@ICG. (A) MC38 tumor tissues with or without treatment were used for RNA-seq analysis. (B) The analysis of the quality control of RNA sequencing. (C) The change in the number of genes after PTT. (D) Significant changes in the expression levels of genes. (E) Changes of many biological processes after PTT. (F) Changes of significant signaling pathways after PTT.

Figure S7

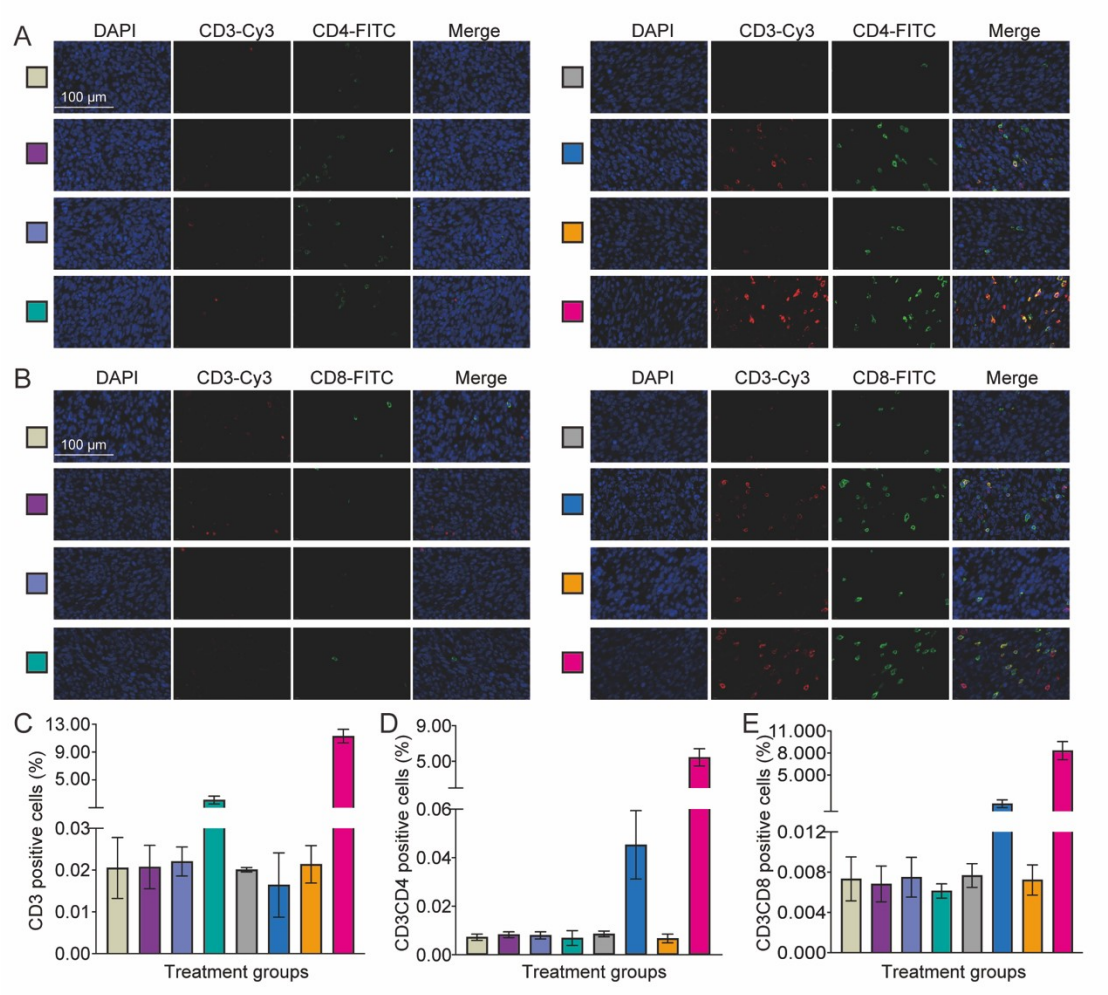

Figure S7. T cells in tumors after different treatments. (A) Representative fluorescent images of CD3+ and CD4+ T cell in tumor tissues. (B) Representative fluorescent images of CD3+ and CD8+ T cell. (C) Quantitative immunofluorescence analysis of positive rate of CD3+ or CD3+CD4+ or CD3+CD8+ T cells in tumor tissues at 12 h after treatments. (n = 3, scale bars = 100 μm).

Figure S8

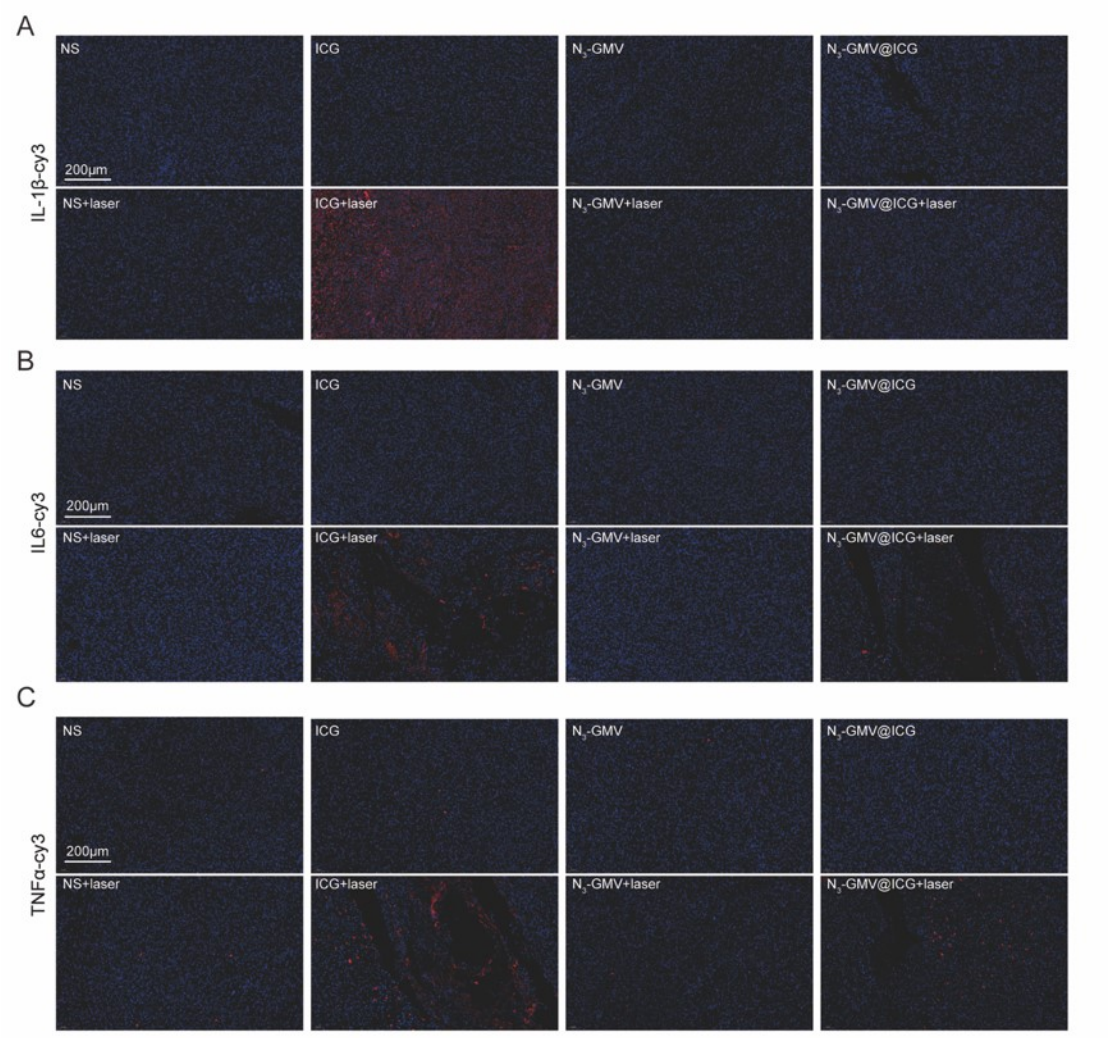

Figure S8. *In vivo* anti-inflammation effect after various treatments. (A-C) The representative immunofluorescence images of IL-1β, IL-6 and TNF-α in tumors. (n=3, scale bars = 200 μm).